Light emitting diodes as an excitation source for biomedical photoacoustics

T. J. Allen and P.C. Beard

Department of Medical Physics and Bioengineering, University College London, Malet Place Engineering Building, Gower Street, WC1E6BT, UK

ABSTRACT

Semiconductor light sources, such as laser diodes or light emitting diodes (LEDs) could provide an inexpensive and compact alternative to traditional Q-switched lasers for photoacoustic imaging. So far, only laser diodes [1–3] operating in the 750 to 905nm wavelength range have been investigated for this purpose. However, operating in the visible wavelength range (400nm to 650nm) where blood is strongly absorbent (>10cm^{-1}) and water absorption is weak (<0.01cm^{-1}) could allow for high contrast photoacoustic images of the superficial vasculature to be achieved. High power laser diodes (>10Watt peak power) are however not available in this wavelength range. High power LEDs could be a potential alternative as they are widely available in the visible wavelength range (400nm to 632nm) and relatively cheap. High power LEDs are generally operated in continuous wave mode and provide average powers of several Watts. The possibility of over driving them by tens of times their rated current when driven at a low duty cycle (<1%), offers the prospect of achieving similar pulse energies (tens of μJ) to that provided by high peak power pulsed laser diodes. To demonstrate the possibility of using high power LEDs as an excitation source for biomedical applications, single point measurements were implemented in a realistic blood vessel phantom. A four colour device was also used to demonstrate the possibility of using LEDs for making spectroscopic measurements. It was shown that when driving all four wavelengths at once, the generated photoacoustic signal could be used to design a filter in order to improve the SNR of the photoacoustic signals generated at each individual wavelength. The possibility of acquiring multiwavelength data sets simultaneously when using Golay excitation methods was also demonstrated. This preliminary study demonstrated the potential for using high power LEDs as an inexpensive and compact excitation source for biomedical photoacoustics.

Keywords: High power LEDs, laser diodes, photoacoustic excitation sources

1. INTRODUCTION

To facilitate the translation of photoacoustic techniques[4] from the laboratory to biomedical applications, cheaper and more compact excitation sources than the traditional Q-switched Nd:YAG pumped OPO, Ti:sapphire or dye laser systems are required. High peak power pulsed laser diodes have previously been investigated as a potential excitation source for photoacoustic tomography[2,3,5]. These devices have the advantage of being compact, relatively inexpensive (<$100), provide high pulse repetition frequencies (>1kHz) and are robust (life times >100000hours). It was shown that their relatively low pulse energy (tens of μJ) compared to the several mJ provided by Q-switched excitation sources could be overcome by exploiting their high pulse repetition frequencies (PRF) to rapidly acquire and signal average many signals over a short period of time. The main drawback of these high peak power pulsed laser diodes is the limited range of wavelengths to select from (905, 850 and 1550nm are the only commercially available wavelengths). Laser diodes in the 500-750nm wavelength range are available but don't provide the necessary high peak powers (>10Watts).

LEDs provide the same advantages as laser diodes with the added benefit of being available in a wider range of wavelength (400-905nm). Figure 1 shows some of the wavelengths that are commercially available. As with laser diodes, the pulse energies provided by LEDs (tens of μJ when overdriven[6,7]) are relatively low compared to those provided by Q-switched excitation sources (several mJ). However, the possibility of exploiting the high PRF of LEDs to rapidly acquire and signal average many signals in a short period of time and the strong absorption of blood in the visible wavelength range (400-750nm) suggest that photoacoustic signals with

Photons Plus Ultrasound: Imaging and Sensing 2013, edited by Alexander A. Oraevsky, Lihong V. Wang,
Proc. of SPIE Vol. 8581, 85811F · © 2013 SPIE · CCC code: 1605-7422/13/$18 · doi: 10.1117/12.2004471

adequate SNR for photoacoustic imaging could be obtained. A previous study using an LED to generate photoacoustic signals has been reported[8]. However in this study, the LED used was only able to provide pulse energies of 360nJ and therefore required the focusing of the emitted light and 50000 signal averages to be implemented in order to detect a photoacoustic signal in a non-realistic phantom.

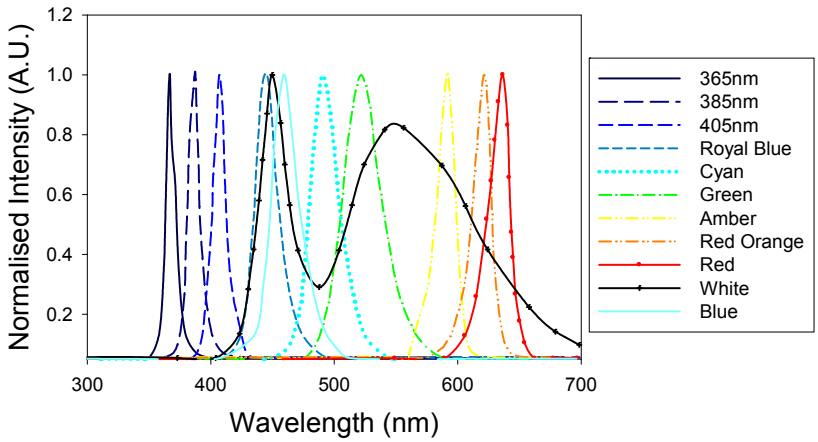

Figure 1: Spectra from typical high power LEDs[9]

In this study LEDs are investigated as a potential excitation source for biomedical photoacoustic applications. Section 2 describes single point measurements made in a realistic tissue mimicking phantom. Section 3 demonstrates the ability of these devices to make spectroscopic measurements and discusses a filtering method used to improve SNR. Section 4 discusses the possibility of using Golay excitation codes to acquire photoacoustic signals at multiple wavelengths simultaneously. Using such excitation codes could reduce the acquisition time when implementing spectroscopic measurements.

2. SINGLE POINT MEASUREMENTS IN A TISSUE MIMICKING PHANTOM

To demonstrate the possibility of using high power LEDs as an excitation source for biomedical photoacoustic applications, a photoacoustic signal was generated and detected in a tissue mimicking phantom. The experimental setup is illustrated in figure 2 where a 580µm diameter tube was filled with human blood (35% haematocrit) and immersed to a depth of 5mm in a 1% solution of intralipid (μ'_s=1mm^{-1}) to mimic the scattering properties of biological tissue. The phantom was illuminated by a high power LED (CBT-120 from Luminus), providing pulse energies of 22µJ when overdriven 10 times its rated current. The excitation pulse duration was 500ns and the PRF was 200Hz. To avoid any thermal damage due to overdriving, the duty cycle was kept below 1%. The emitting wavelength was 623nm and the beam diameter incident on the scattering medium was approximately 1cm in diameter. The generated photoacoustic signal was detected using a cylindrically focused PZT detector (3.5MHz, V383 Panametric) of focal length 33mm. The blood filled tube was located at the focus of the ultrasound detector. The detected signal was amplified using a preamplifier (8dB, Precision Acoustics Ltd) and a low noise voltage amplifier (60dB, Analog Modules Inc), signal averaged 1000 times and then downloaded to a personal computer (PC).

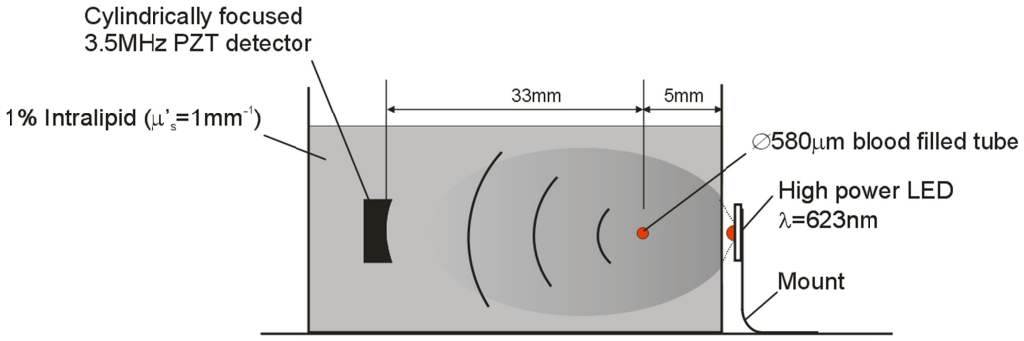

Figure 2: Experimental setup, composed of 580μm diameter blood filled tube immersed in a solution of intralipid (μ'$_s$=1mm^{-1})

Figure 3 shows an example of a photoacoustic signal obtained from the setup show in figure 2. A reflection of the photoacoustic signal arises at the interface between the intralipid and the wall of the tank and can been seen at time=30μs. The SNR of the photoacoustic signal was measured to be 13.

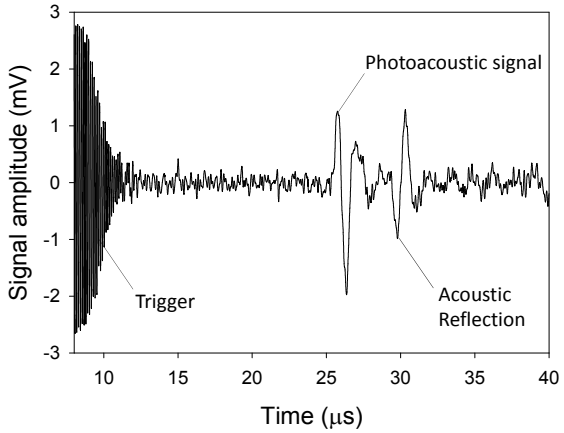

Figure 3: Photoacoustic signal generated in a realistic tissue mimicking phantom

3. SPECTROSCOPIC MEASUREMENTS

Several LEDs of different wavelengths can be densely packed in a single package making them ideal for photoacoustic spectroscopy. For example, the LZC-A0MA40 from LedEngin is composed of 12 LEDs, emitting at four wavelengths (460, 523, 590 and 623nm) with a total footprint of 9mm^2. Each of these four wavelengths can be driven individually or all at once. To demonstrate the spectroscopic capability of this device, photoacoustic signals were generated in a solution of methylene blue for each of the four wavelengths. Methylene blue is here chosen as its absorption spectrum is well known.

The experimental setup shown in figure 4 is composed of a cuvette filled with methylene blue (μ_a=20mm^{-1} at λ=600nm) and immersed to a depth of 5mm in water. The cuvette was illuminated in turns by each of the four wavelengths. Pulse energies of 3.6, 0.7, 1.4, 2μJ were obtained when emitting at 460, 523, 590 and 623nm respectively and overdriving the LEDs by ten times their rated current. The excitation pulse duration was 500ns and the PRF was 200Hz. To avoid thermal damage occurring to the device, due to overdriving, the duty cycle was kept below 1%. The beam diameter incident on the scattering medium was approximately 1cm in diameter. The generated photoacoustic signals were detected using a planar PZT detector (3.5MHz, V381 Panametric).

The signals were them amplified using a low noise voltage amplifier (Femto, 40dB), signal averaged 1000 times and then downloaded to a PC.

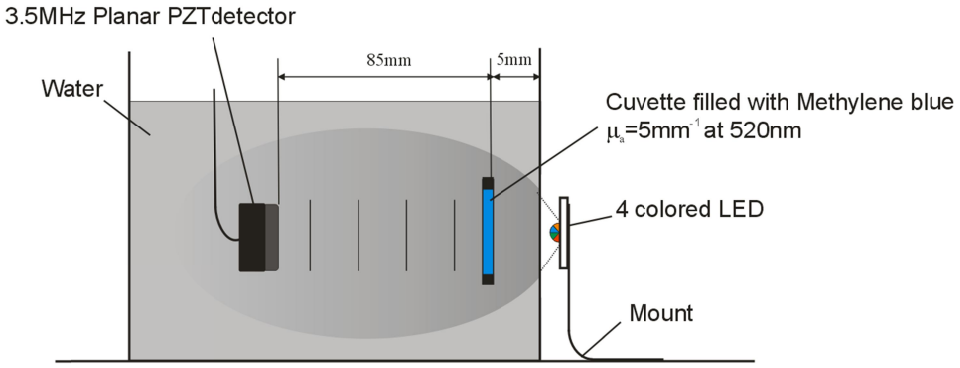

Figure 4: Experimental setup, consisting a cuvette filled of Methylene blue immersed in water

Figure 5 (a-d) shows the photoacoustic signals generated in the cuvette of methylene blue when emitting at a wavelength of 460, 523, 590 and 623nm respectively. A reflection of the photoacoustic signal arises at the interface between the water and the wall of the tank and can be seen at time=75μs. The low amplitude of the photoacoustic signal generated when illuminating at 523nm is a results of the relatively low pulse energy (0.7µJ) provided at that wavelength and of the weak absorption coefficient of methylene blue.

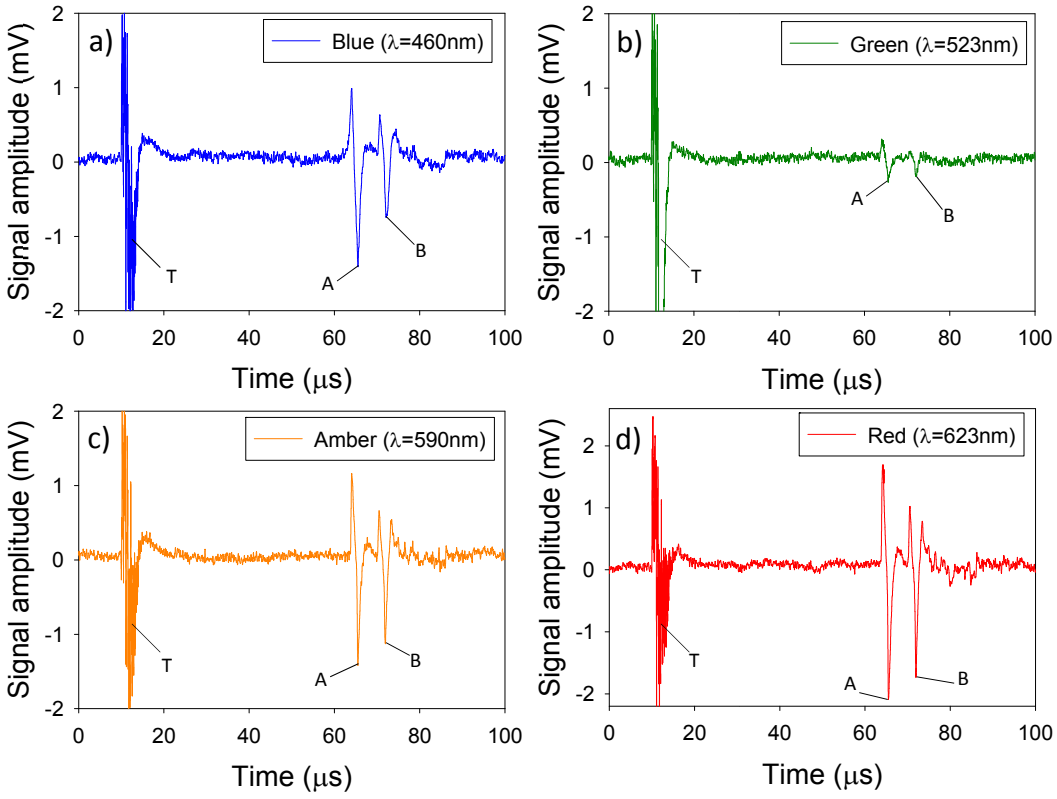

Figure 5: Photoacoustic signals generated at (a) 460nm, (b) 523nm, (c) 590nm and (d) 623nm, where T is the trigger, A is the photoacoustic signal and B is an acoustic reflection.

The four colour device provides the possibility of driving all four of its wavelengths simultaneously allowing for a photoacoustic signal with improved SNR to be acquired. For example, the photoacoustic signal shown in figure 6 was obtained using the setup shown in figure 4 when all wavelengths are driven simultaneously. The SNR of this photoacoustic signal was measurement to be 71 as opposed 21, 6, 30, and 32 obtained when individually emitting at a wavelength of 460, 523, 590, and 623nm respectively.

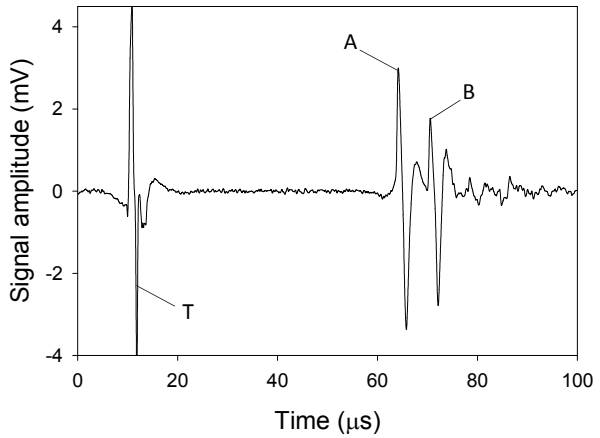

Figure 6: Photoacoustic signal obtained when driving all four wavelength simultaneously. T is the trigger, A is the photoacoustic signal and B is an acoustic reflection.

If it is assumed that the temporal shape of the photoacoustic signals generated by each individual wavelength are identical to each other (this is reasonable when the light penetration depth is significantly larger than the size of the absorber), the power spectrum of the photoacoustic signal generated by all wavelengths simultaneously can be used to design a filter to improve the SNR of the photoacoustic signals generated by each individual wavelength.

This can be implemented as a wiener filter (*H(f)*)

$$H(f) = \frac{\left|S_{\lambda_{all}}(f)\right|^2}{\left|S_{\lambda_{all}}(f)\right|^2 + N} \quad (1)$$

Where $\left|S_{\lambda_{all}}(f)\right|^2$ is the power spectrum of the photoacoustic signal generated by all 4 wavelengths and N is the threshold in the power spectrum where noise becomes dominant. The photoacoustic signals generated by a single wavelength ($S_{\lambda 1}$) can then be filtered as follow

$$Y_{\lambda_1}(t) = IFFT[FFT(S_{\lambda_1}(t)) \times H(f)] \quad (2)$$

where $S_{\lambda 1}$ and $Y_{\lambda 1}$ are the photoacoustic signals generated by a single wavelength before and after filtering. Figure 7 shows the photoacoustic signals previously show in figure 5 after filtering. An improvement in the SNR by a factor of 3 was observed.

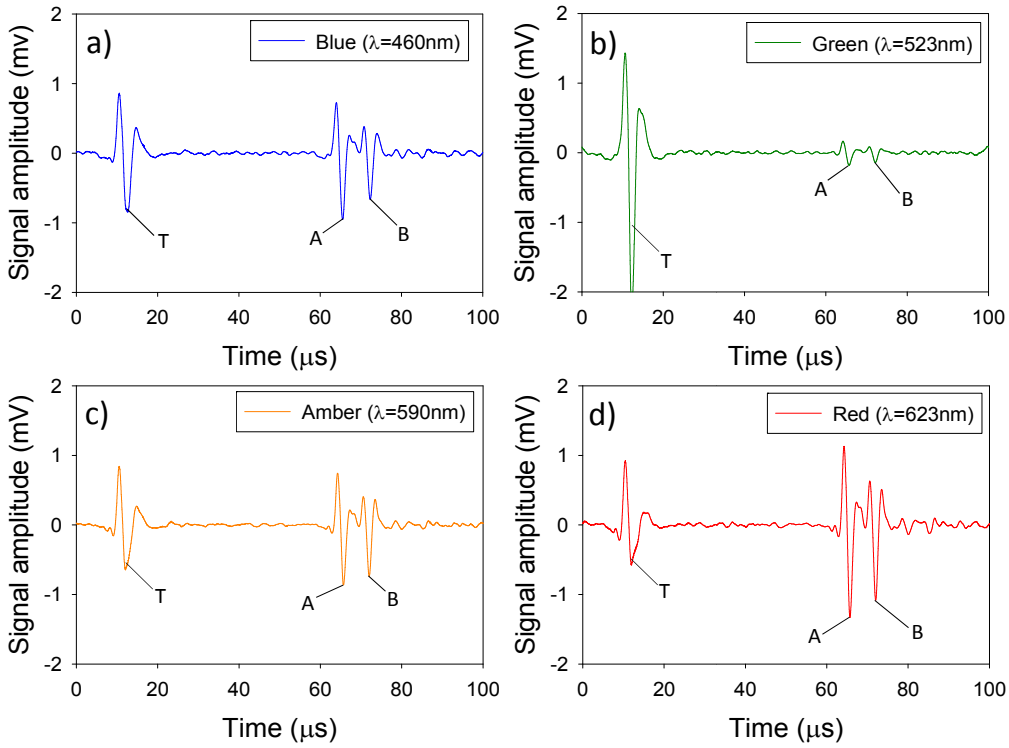

Figure 7: Photoacoustic signals generated at (a) 460nm, (b) 523nm, (c) 590nm and (d) 623nm after filtering. T is the trigger, A is the photoacoustic signal and B is an acoustic reflection.

4. GOLAY EXCITATION METHOD

LEDs have the advantage compared to traditional excitation sources such as Q-switched Nd:YAG lasers that they can be arbitrarily modulated allowing for coded excitation schemes such as Golay codes to be implemented. Golay excitation methods require that two biphase codes (e.g. A and B), with code symbols ±1 to be transmitted[10,11]. Biphase codes are generated in photoacoustics by transmitting two unipolar codes representing the +1 (e.g. A_p for code A and B_p for code B, see figure 8) and -1 (e.g. A_n for code A and B_n for code B), the generated photoacoustic signals (P_{Ap} and P_{An} for code A and P_{Bp} and P_{Bn} for code B) are then subtracted from one and another (e.g. P_{Ap}-P_{An} and P_{Bp}-P_{Bn}). The desired signal is then obtained by cross correlating the biphase codes with their respective photoacoustic signals and summing them up ($(A_p\text{-}A_n)\star(P_{Ap}\text{-}P_{An})+(B_p\text{-}B_n)\star(P_{Bp}\text{-}P_{Bn})$). This requires that a total of four sequences to be transmitted to acquire a whole data set (see figure 8).

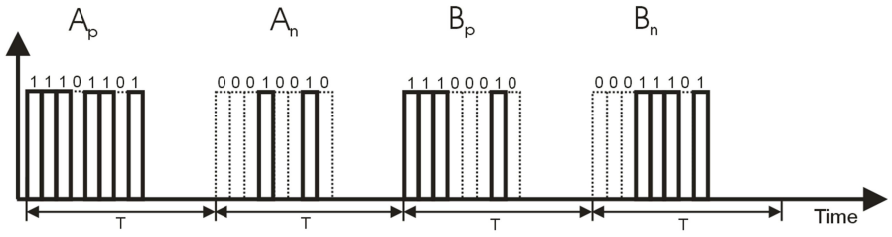

Figure 8: Example of a 8bit long Golay excitation code used for photoacoustic generation. Four modulated pulses are transmitted. The first two pulses are modulated with the sequences A_p and A_n representing the positive (1) and negative (-1) bits of the biphase code A of the Golay code. The second two pulses are modulated with the sequences B_p and B_n represent the positive (1) and negative (-1) bit of the biphase code B. T is the time delay between consecutive pulses.

Golay codes have two main advantages; (1) they allow for the SNR of the photoacoustic signal to be increased as a function of $\sqrt{N}$ where N is the code length, (2) they can be used to acquire a data set at multiple wavelengths simultaneously[12] when using different sets of orthogonal codes. To illustrate the latter, the experimental setup shown in figure 4 was used to generate photoacoustic signals whiles driving the 460nm and 590nm device with two different sets of orthogonal codes simultaneously. The code was 8bit long and each bit was 1μs long corresponding to a total duration of 8μs.The PRF of the LEDs was 200Hz. The devices were here only overdriven by three times their rated current to prevent from any damage due to the increased duty cycle.

Figure 9 (a) and (b) show the photoacoustic signals obtained using the Golay excitation method (emitting both wavelengths simultaneously) and the conventional pulsed excitation method (emitting each wavelength sequentially) respectively. It can be seen that the temporal shapes of the photoacoustic signals obtained using the Golay excitation method correlate well with those obtained using the pulsed excitation method. The main observable differences is the noise level being significantly reduced in figure 9 (a) compared to figure 9 (b). The reduction in noise is due to the cross correlation acting as a low pass filter, removing the unnecessary high frequency components which are dominated by noise. The bandwidth of the photoacoustic signal generated by the Golay excitation method is determined by the width of each bit (1μs). The acquisition time was 20ms when using the Golay excitation method whereas for the pulsed excitation method an acquisition time of 80ms was required when operating at a PRF=200Hz.

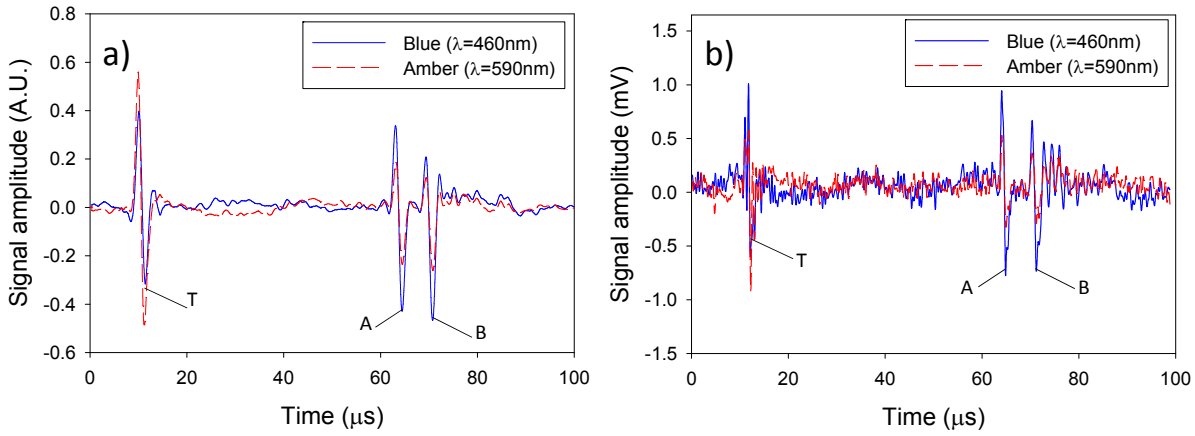

Figure 9: (a) Photoacoustic signals generated using Golay excitation codes (b) Photoacoustic signals generated by pulsed excitation method. T is the trigger, A is the photoacoustic signal and B is an acoustic reflection.

5. DISCUSSION & CONCLUSION

This study has demonstrated that high power LEDs could be used to generate photoacoustic signals with sufficient SNR to achieve penetrations depths of 5mm in a realistic blood vessel phantom. By exploiting the high absorption coefficient of blood in the visible wavelength range and the high PRF of the LEDs to acquire and signal average many signals over a short period of time adequate SNR was obtained with pulse energis of a few μJ. Improvements in SNR could potentially be obtained by further overdriving these devices. For example, the CBT-120 device was only overdriven by 10 times its rated current, as the maximum peak current provided by the driver was limited to 200A. However, it has been reported[6] that this device can withstand peak currents of up to 250A. A detailed study investigating the amount of overdriving these LEDs can withstand and the effect this will have on their lifespan is required.

The possibility of acquire photoacoustic signal at multiple wavelengths simultaneously when using Golay codes was also demonstrated. The SNR of the photoacoustic signal acquired using this excitation method could be

improved if longer excitation codes were used, as the SNR will scale with $\sqrt{N}$. Increasing the code length will limit the amount of overdriving which can be implemented safely as the junction temperature of the LED will rise due to the increase in duty cycle. However if the code length is made sufficient long (e.g. >10000bits) it may not be necessary to overdrive the LEDs in order to obtain photoacoustic signals with adequate SNR. Such an excitation scheme has the potential to reduce the acquisition time when implementing photoacoustic spectroscopic measurements.

So far the LEDs have been placed as close as possible to the tissue mimicking phantoms and the beam diameter illuminating the sample has been relatively large (1cm) due to the large size of the emitting area $12mm^2$ and the divergence (60^o) of the light. It may be possible to weakly collimate the light on to the phantom. This could result in an improvement in the SNR of the generated photoacoustic signal due to the increase in fluence. In addition if sufficient focusing can be achieved these devices may be suitable for imaging modalities which require relatively low pulse energies, such as acoustic resolution photoacoustic microscopy (ARPAM) which requires pulse energies of tens of μJ[13] or optical resolution photoacoustic microscopy (ORPAM) where pulse energies of less than $100nJ$[14,15] are required.

In summary this work represents a first step towards demonstrating that high power LEDs could be used as a compact and relatively low cost excitation source for superficial biomedical photoacoustic applications.

REFERENCES

1. Maslov, K. & Wang, L. V. Photoacoustic imaging of biological tissue with intensity-modulated continuous-wave laser. *Journal of Biomedical Optics* **13**, 024006 (2005).

2. Allen, T. J. & Beard, P. C. Pulsed near-infrared laser diode excitation system for biomedical photoacoustic imaging. *Optics Letters* **31**, 3462–4 (2006).

3. Kolkman, R. G. M., Steenbergen, W. & van Leeuwen, T. G. In vivo photoacoustic imaging of blood vessels with a pulsed laser diode. *Lasers in Medical Science* **21**, 134–9 (2006).

4. Beard, P. Biomedical photoacoustic imaging. *Interface Focus* **1**, 602–631 (2011).

5. Allen, T. J. & Beard, P. C. Dual wavelength laser diode excitation source for 2D photoacoustic imaging. *Proceedings of SPIE* **6437**, 64371U–64371U–9 (2007).

6. Willert, C., Stasicki, B., Klinner, J. & Moessner, S. Pulsed operation of high-power light emitting diodes for imaging flow velocimetry. *Measurement Science and Technology* **21**, 075402 (2010).

7. Willert, C. E., Mitchell, D. M. & Soria, J. An assessment of high-power light-emitting diodes for high frame rate schlieren imaging. *Exp Fluids* **53**, 413–421 (2012).

8. Skov Hansen, R. Using high-power light emitting diodes for photoacoustic imaging. *Proceedings of SPIE* **7968**, 79680A–79680A–6 (2011).

9. Mightex Mightex LED Typical Spectra. http://www.mightexsystems.com

10. Mienkina, M. *et al.* Experimental evaluation of photoacoustic coded excitation using unipolar golay codes. *Ieee Transactions on Ultrasonics Ferroelectrics and Frequency Control* **57**, 1583–93 (2010).

11. Chiao, R. Y. & Hao, X. Coded excitation for diagnostic ultrasound: a system developer's perspective. *Ieee Transactions on Ultrasonics Ferroelectrics and Frequency Control* **52**, 160–70 (2005).

12. Mienkina, M. P. *et al.* Multispectral photoacoustic coded excitation imaging using unipolar orthogonal Golay codes. *Optics Express* **18**, 9076–87 (2010).

13. Zhang, H. F., Maslov, K., Stoica, G. & Wang, L. V. Functional photoacoustic microscopy for high-resolution and noninvasive in vivo imaging. *Nature Biotechnology* **24**, 848–51 (2006).

14. Song, L., Maslov, K. & Wang, L. V. Multifocal optical-resolution photoacoustic microscopy in vivo. *Optics Letters* **36**, 1236–8 (2011).

15. Wang, L. L. V., Maslov, K., Yao, J. & Rao, B. Fast voice-coil scanning optical-resolution photoacoustic microscopy. *Optics Letters* **36**, 139–41 (2011).